Proximity effect between an unconventional superconductor and a ferromagnet with spin bandwidth asymmetry

Mario Cuoco,[1,2] Alfonso Romano,[1,2] Canio Noce,[1,2] and Paola Gentile[1,3]
[1]*Laboratorio Regionale SuperMat, CNR-INFM, Baronissi, Salerno, Italy*
[2]*Dipartimento di Fisica "E. R. Caianiello," Università di Salerno, I-84081 Baronissi, Salerno, Italy*
[3]*International School for Advanced Studies (SISSA) and INFM Democritos National Simulation Center, via Beirut 2-4, I-34014 Trieste, Italy*
(Received 14 March 2008; revised manuscript received 19 June 2008; published 8 August 2008)

We study the proximity effect within a junction made of an unconventional superconductor (US) and a ferromagnet (F) in the clean limit with high barrier transparency. Superconductivity in the US side is described by an extended Hubbard model with intersite attractive interaction, while metallic ferromagnetism in the F side is assumed to be originated by a relative change in the bandwidths of electrons with opposite spin. The effect of this mass-split mechanism is analyzed in conjunction with the usual Stoner-like one, where one band is rigidly shifted with respect to the other, due to the presence of a constant exchange field. Starting from the numerical solution of the Bogoliubov-de Gennes equations, we show that the two above mentioned mechanisms for ferromagnetism lead to different features as concerns the formation at the interface of dominant and subdominant superconducting components, as well as their propagation in the ferromagnetic side. This considerably affects the opening of gaplike structures in the local density of states for majority and minority spin electrons, leading to distinct effects as one moves toward the half-metallic regime, where the density of the minority carriers becomes vanishing.

DOI: 10.1103/PhysRevB.78.054503 PACS number(s): 74.45.+c, 74.20.Rp, 74.78.Fk

I. INTRODUCTION

The conventional proximity effect between a superconductor (S) and a normal (N) metal brought into contact is the penetration of the superconducting condensate in the N layer over a distance significantly exceeding the interatomic spacing.[1] The phenomenon is largely dominated by a fundamental transport process through the interface, the so-called Andreev reflection,[2] by which an electron with energy below the superconducting gap is reflected as a hole and a Cooper pair is transmitted into the superconductor. Andreev reflection thus provides the basic mechanism allowing a dissipative quasi-particle current in the normal metal to be transferred as a supercurrent with no dissipation in the superconductor.

When the normal metal is replaced by a ferromagnet (F), there is again a penetration of the pair wave function in the F side, but two fundamental differences arise with respect to the $N-S$ case:[3,4] (i) the penetration depth of the superconducting condensate is considerably reduced by the pair breaking effect due to the exchange field tending to align spins in the Cooper pair, and (ii) the relative shift of the electronic band of the two spin species makes the wave vectors of two paired electrons different, so that the pair acquires a finite momentum and, correspondingly, its wave function oscillates in space in the ferromagnetic layer. These features give rise to relevant effects, now repeatedly observed in experiments, such as a nonmonotonic dependence of the critical temperature of S/F multilayers on the F layer thickness,[5] as well as the possible realization of Josephson $S/F/S$ π junctions[6] characterized by an equilibrium phase difference between the two superconducting layers equal to π and not to zero as it happens in the standard $S/N/S$ case.

Even more specific features emerge when the proximity involves an unconventional superconductor (US) with anisotropic pairing, rather than a system characterized by a k-independent s-wave symmetry of the order parameter. This topic has become of particular relevance in the last years, given the large experimental evidence that anisotropic superconductivity is realized in several classes of materials, such as high-T_c superconducting oxides, heavy-fermion compounds, ruthenates, and quasi-one-dimensional organic systems. New effects are associated in this case with the phenomenon of the Andreev reflection. In particular, when the pair potential becomes anisotropic and changes sign across the Fermi surface, the specific interference taking place between incident and reflected quasiparticles can originate zero-energy Andreev bound states at the surface,[7–9] as a consequence of the potential wells caused by the inhomogeneity of the pair potential. These bound states are responsible for the zero-bias conductance peak observed in tunneling spectroscopy experiments performed on many of the systems mentioned above, such as the high-T_c oxide $YBa_2Cu_3O_{7-\delta}$,[10] the ruthenate Sr_2RuO_4,[11] and the heavy-fermion system UBe_{13}.[12] Recent theoretical investigations have also pointed out some relevant differences occurring in transport properties depending on whether the pairing symmetry is the singlet d-wave[13] or the triplet p-wave one.[14] This issue has been deeply investigated in particular in the diffusive limit, referring specifically to junctions made with singlet[15] and triplet[16] superconductors. Moreover, the different response seen in tunneling experiments in the presence of an external magnetic field has also been proposed as a valuable tool to distinguish among the two kinds of symmetries.[17]

On the other hand, when in a junction with an unconventional superconductor the normal metallic layer is replaced by a ferromagnet, further peculiar effects are detected. Indeed, the presence of an exchange field in the F part, com-

 ©2008 The American Physical Society

bined with the effect of the Fermi wave-vector mismatch associated with the different bandwidths in the two junction materials, modifies the Andreev reflections at the interface in a nontrivial way.[18–22] Theoretical predictions for the case of a *d*-wave superconductor indicate that this can affect transport properties in a variety of ways, so that the zero-bias conductance peak seen in the $N-S$ case can split into two peaks[18,20,23] or rather it can be replaced by a dip or even move to finite energies.[19]

The effects introduced by the presence in $N-S$ and $F-S$ heterostructures of unconventional superconductors with a nontrivial angular dependence of the pair wave function have been deeply investigated, both from a theoretical and an experimental point of view, in a large number of papers published in the last years.[24] In order to investigate new effects concerning the above mentioned issues, we analyze in this paper proximity phenomena between an unconventional superconductor and a ferromagnetic system, in the case where the magnetization in the F side can be due either to a standard Stoner-like mechanism originated by the presence of an exchange field (which can be intrinsic or external), or to an asymmetry between the hopping amplitudes for electrons with opposite spins, which produces a relative change in the bandwidths for the two spin species. When moving toward the half-metallic regime, where the density of the minority carriers tends to zero, each of the two mechanisms becomes of special relevance for the description of distinct classes of real ferromagnets.[25,26]

As far as ferromagnetism due to spin bandwidth asymmetry is concerned, a possible microscopic origin is the well-known double exchange mechanism originating from spin pairing caused by the Hund's rule within degenerate orbitals.[27] This forces atoms to be in the configuration with the highest possible spin value, thus favoring the itinerancy of electrons with a given spin projection and the concomitant tendency to localization of the electrons in the opposite spin state. This different kinetic energy renormalization occurring to opposite spin electrons can be looked at as an asymmetric effective mass renormalization or, equivalently, as a relative bandwidth variation. A different mechanism ultimately leading to the same situation is the one based on the mass undressing for majority spins proposed by Hirsch.[28] It is suggested that certain off-diagonal terms that arise in deriving a Hubbard-like tight-binding Hamiltonian from first-principles calculations, generally neglected in studies based on the Hubbard model, are likely to play a fundamental role in the possible occurrence of metallic ferromagnetism. The mean-field treatment of a generalization of the Hubbard model including the most relevant of these contributions, the so-called exchange and pair hopping terms, has shown that as the temperature is lowered, it becomes energetically advantageous for the system to acquire a spin polarization, with a gain in kinetic energy associated with the increase in the bandwidth of the majority spin species with respect to the minority one. Therefore, within this picture the ferromagnetism should be understood as kinetically driven, in the sense that differently from what happens in the usual Stoner scheme, it arises from a gain in kinetic rather than potential energy. Finally, we notice that this mass-split metallic ferromagnetism has been experimentally found to be at the origin of the optical properties of the colossal magnetoresistance manganites,[29] of some rare-earth hexaborides,[30] as well as of some magnetic semiconductors.[31]

In our approach the system is described in terms of an extended Hubbard model in real space, which is solved via a microscopic mean-field self-consistent calculation based on the numerical solution of the Bogoliubov-de Gennes equations. We show that the two mechanisms for ferromagnetism give rise to nontrivial differences in the behavior of the $F-S$ junction. They mainly concern the formation at the interface of dominant and subdominant superconducting components with singlet and triplet symmetry, as well as their oscillating propagation in the ferromagnetic side. These features are shown to be of special relevance in determining the behavior of the local electronic densities of states for majority and minority spin carriers, affecting in particular the opening of gaplike structures associated with the electron pairing in the different possible symmetry channels.

The study is performed considering a model junction in two dimensions, in the limit of high interface transparency. Apart from the intrinsic theoretical interest inherent in this limit, this analysis can turn out to be of relevance in connection with recent studies on the eutectic system Sr_2RuO_4-$Sr_3Ru_2O_7$, where an internal anomalous proximity effect is induced in the $Sr_3Ru_2O_7$ component by Sr_2RuO_4 superconducting macrodomains.[32] All the calculations have been developed under the assumption of a nearest-neighbor hopping amplitude on both the F and the S side. The effects introduced by the specific features of the corresponding energy spectrum, characterized by a van Hove singularity in the bare density of states, are fully taken into account and shown to play a relevant role in the characterization of the electronic states at the interface, as well as in the determination of the peculiar features characterizing the behavior of the local densities of states for the two spin species.

The paper is organized as follows. In Sec. II we introduce the model used to describe the $F-S$ junction and present the technique of solution of the related Bogoliubov-de Gennes equations. In Sec. III we discuss the results obtained for the propagation of the order parameters in the various symmetry channels, referring to the two cases of a superconductor with bulk p_x+ip_y and *d*-wave symmetry. Section IV is devoted to the analysis of the local densities of states for majority and minority spin carriers, with a special attention to the distinct effects introduced by the two different mechanisms for ferromagnetism considered here. Section V is devoted to the conclusions.

II. MODEL AND FORMALISM

The system is basically constituted by a two-dimensional bilayer with a ferromagnetic and a superconducting part separated by an interface. In the following, we assume that the direction perpendicular (parallel) to the interface is denoted as $x(y)$, and that the system is uniform along the y-axis direction. The microscopic model is represented by an extended Hubbard model on a square lattice that we treat within the Hartree-Fock approximation to describe magnetism and superconductivity at zero temperature.

In standard approaches, such as those based on the Stoner model, metallic ferromagnetism is due to a rigid shift in the positions of majority and minority spin bands due to the self-consistent exchange field associated with opposite spin electrons. A relevant feature of our study is the consideration that besides being possibly generated by a Stoner-like mechanism, ferromagnetism can also develop as a consequence of a change in the relative bandwidth of electrons with up and down spin polarization, leading to a lowering of the total kinetic energy of the system.[28] This novel mechanism has recently been shown to support, under suitable conditions, the coexistence of s-wave singlet superconductivity and ferromagnetism in a single band model.[33]

We will thus be specifically interested in the case where a side of the junction, say, the right one, is an unconventional superconductor, while the other side is a ferromagnet with possible spin-dependent electron itinerancy. The total Hamiltonian of the system is correspondingly written in the form

$$H = H_F + H_S + H_T, \tag{1}$$

where H_F and H_S refer to the F and S layers, respectively, whereas H_T defines the coupling between the two sides of the junction. The explicit form of the Hamiltonians H_F and H_S is

$$H_A = -\sum_{\langle \mathbf{i},\mathbf{j}\rangle,\sigma} t_{A\sigma}(c^{\dagger}_{\mathbf{i}\sigma}c_{\mathbf{j}\sigma} + \text{h.c.}) + \sum_{\mathbf{i}} U_A n_{\mathbf{i}\uparrow}n_{\mathbf{i}\downarrow} + \sum_{\langle \mathbf{i},\mathbf{j}\rangle} V_A(n_{\mathbf{i}\uparrow}n_{\mathbf{j}\downarrow} + n_{\mathbf{i}\downarrow}n_{\mathbf{j}\uparrow}) - \mu\sum_{\mathbf{i},\sigma} n_{\mathbf{i}\sigma} - h_A\sum_{\mathbf{i},\sigma}(n_{\mathbf{i}\uparrow} - n_{\mathbf{i}\downarrow}) \quad A = F,S, \tag{2}$$

where $\langle \mathbf{i},\mathbf{j}\rangle$ denotes nearest-neighbor sites, $c_{\mathbf{i}\sigma}$ is the annihilation operator of an electron with spin σ at site $\mathbf{i}\equiv(i_x,i_y)$, and $n_{\mathbf{i}\sigma}=c^{\dagger}_{\mathbf{i}\sigma}c_{\mathbf{i}\sigma}$ is the corresponding number operator. The magnetic field, which in this context can be equivalently seen either as an external or an intrinsic one, is assumed to be nonvanishing only in the F side ($h_F\neq 0$, $h_S=0$) while for the hopping amplitudes we choose $t_{S\uparrow}=t_{S\downarrow}\equiv t_S$, with the possibility of having $t_{F\uparrow}\neq t_{F\downarrow}$. This implies that, besides being possibly originated by a standard exchange field h_F, ferromagnetism can be due to a spin dependence of the hopping amplitude, such that the majority spin electrons have a larger bandwidth compared to the minority spin ones. Moreover, μ is the common chemical potential, the parameter U_A ($A=F,S$) represents the on-site repulsion for the A side (U_F, $U_S>0$), whereas the nearest-neighbor attraction V_A is chosen to be nonvanishing only on the S side ($V_F=0$, $V_S<0$). In this way, the possibility of isotropic pairing between electrons on the same site has been excluded from the very beginning.

Finally, the coupling between the two sides of the junction is ensured by the term H_T, which describes the transmission of electrons at the interface. It is given by

$$H_T = -t_T\sum_{\langle \mathbf{lm}\rangle\sigma}(c^{\dagger}_{\mathbf{l}\sigma}c_{\mathbf{m}\sigma} + \text{H.c.}), \tag{3}$$

where $\mathbf{l}(\mathbf{m})$ denotes sites at the surface for the left (right) layer.

We point out that in the present treatment spin-flip interfacial scattering effects are ignored. However, in the case of junctions involving a ferromagnet, this type of scattering may be important[34] and one should thus introduce a corresponding new term into the Hamiltonian. Indeed, since the spin-flip mechanism tends to spoil the preoriented spin direction of conduction electrons incident from the ferromagnet, it seriously influences the conductance spectrum. In particular, the splitting of the zero-bias conductance peaks induced by the exchange field is in this case washed out, giving rise to a conductance spectrum completely structureless. Furthermore, the same mechanism reduces the tendency to the suppression of the conductance in the region away from zero bias due to the presence of an exchange field.

The interaction terms in H_F and H_S are decoupled by means of a standard Hartree-Fock approximation such that the magnetic and the pairing channels originate from the on-site and the intersite interactions, respectively:

$$Un_{\mathbf{i}\uparrow}n_{\mathbf{i}\downarrow} \simeq U[\langle n_{\mathbf{i}\downarrow}\rangle n_{\mathbf{i}\uparrow} + \langle n_{\mathbf{i}\uparrow}\rangle n_{\mathbf{i}\downarrow} - \langle n_{\mathbf{i}\uparrow}\rangle\langle n_{\mathbf{i}\downarrow}\rangle],$$

$$Vn_{\mathbf{i}\uparrow}n_{\mathbf{j}\downarrow} \simeq V[\Delta_{\mathbf{ij}}c^{\dagger}_{\mathbf{j}\downarrow}c^{\dagger}_{\mathbf{i}\uparrow} + \Delta^{*}_{\mathbf{ij}}c_{\mathbf{i}\uparrow}c_{\mathbf{j}\downarrow} - |\Delta_{\mathbf{ij}}|^2].$$

Here we have introduced the pairing amplitude on a bond $\Delta_{ij}=\langle c_{\mathbf{i}\uparrow}c_{\mathbf{j}\downarrow}\rangle$, with the average $\langle K\rangle$ indicating the expectation value of the operator K over the ground state. Hence, Δ_{ij} and the on-site magnetization $m_{\mathbf{i}}=\frac{1}{2}(\langle n_{\mathbf{i}\uparrow}\rangle-\langle n_{\mathbf{i}\downarrow}\rangle)$ are the order parameters (OPs) to be determined self-consistently. From the pairing amplitudes Δ_{ij}, it is possible to build the superconducting OPs for the different crystal symmetries in the singlet (S) and triplet (T) channel for the zero component of the projected axial spin operator. They are defined as

$$\Delta_s(\mathbf{i}) = [\Delta^{(S)}_{\mathbf{i},\mathbf{i}+\hat{\mathbf{x}}} + \Delta^{(S)}_{\mathbf{i},\mathbf{i}-\hat{\mathbf{x}}} + \Delta^{(S)}_{\mathbf{i},\mathbf{i}+\hat{\mathbf{y}}} + \Delta^{(S)}_{\mathbf{i},\mathbf{i}-\hat{\mathbf{y}}}]/4,$$

$$\Delta_d(\mathbf{i}) = [\Delta^{(S)}_{\mathbf{i},\mathbf{i}+\hat{\mathbf{x}}} + \Delta^{(S)}_{\mathbf{i},\mathbf{i}-\hat{\mathbf{x}}} - \Delta^{(S)}_{\mathbf{i},\mathbf{i}+\hat{\mathbf{y}}} - \Delta^{(S)}_{\mathbf{i},\mathbf{i}-\hat{\mathbf{y}}}]/4,$$

$$\Delta p_x(\mathbf{i}) = [\Delta^{(T)}_{\mathbf{i},\mathbf{i}+\hat{\mathbf{x}}} - \Delta^{(T)}_{\mathbf{i},\mathbf{i}-\hat{\mathbf{x}}}]/2,$$

$$\Delta p_y(\mathbf{i}) = [\Delta^{(T)}_{\mathbf{i},\mathbf{i}+\hat{y}} - \Delta^{(T)}_{\mathbf{i},\mathbf{i}-\hat{\mathbf{y}}}]/2$$

for extended s, $d_{x^2-y^2}$, p_x, and p_y wave, respectively. Here we have introduced the singlet and triplet pairing amplitudes on a bond, given by

$$\Delta^{S}_{\mathbf{ij}} = (\Delta_{\mathbf{ij}} + \Delta_{\mathbf{ji}})/2,$$

$$\Delta^{T}_{\mathbf{ij}} = (\Delta_{\mathbf{ij}} - \Delta_{\mathbf{ji}})/2.$$

Moreover, we introduce for convenience the following notation:

$$\Delta^{\mathbf{x}\pm}_{\mathbf{i}} = \Delta_{\mathbf{i},\mathbf{i}\pm\hat{\mathbf{x}}},$$

$$\Delta^{\mathbf{y}\pm}_{\mathbf{i}} = \Delta_{\mathbf{i},\mathbf{i}\pm\hat{\mathbf{y}}}.$$

We adopt open (periodic) boundary conditions for the direction x perpendicular (y parallel) to the interface, taking the Fourier transform along the y direction of the relevant physical quantities. With such conditions and within the mean-field approximation it is possible to rewrite the Hamiltonian in the form[35]

$$H_{\mathrm{MFA}} = \sum_{\mathbf{k}} \sum_{\mathbf{i},\mathbf{j}} D_{\mathbf{i}}^{\dagger}(\mathbf{k}) h_{\mathbf{ij}}(\mathbf{k}) D_{\mathbf{j}}(\mathbf{k}), \tag{4}$$

where $\mathbf{k}$ is the wave vector for the direction parallel to the interface and the vector $D_{\mathbf{i}}^{\dagger}(\mathbf{k})$ is defined as $D_{\mathbf{i}}^{\dagger}(\mathbf{k}) = [c_{\mathbf{i}\uparrow}^{\dagger}(\mathbf{k}), c_{\mathbf{i}\downarrow}(-\mathbf{k})]$. Moreover, the matrix $h_{\mathbf{ij}}$ is

$$h_{\mathbf{ij}} = \begin{bmatrix} \varepsilon_{\mathbf{ij}\uparrow}(\mathbf{k}) & F_{\mathbf{ij}}(\mathbf{k}) \\ F_{\mathbf{ij}}^{*}(\mathbf{k}) & -\varepsilon_{\mathbf{ij}\downarrow}(\mathbf{k}) \end{bmatrix},$$

where

$$\varepsilon_{\mathbf{ij}\sigma}(\mathbf{k}) = [-2t_{\mathbf{ij}\sigma}\cos(\mathbf{k}a) - \mu + U\langle n_{\mathbf{i},-\sigma}\rangle - \sigma h_{\mathbf{i}}]\delta_{\mathbf{ij}} - t_{\mathbf{ij}\sigma}[\delta_{\mathbf{i},\mathbf{j}+\mathbf{a}} + \delta_{\mathbf{i},\mathbf{j}-\mathbf{a}}],$$

$$F_{\mathbf{ij}}(\mathbf{k}) = -V_{\mathbf{ij}}[\Delta_{\mathbf{i}}^{x+}\delta_{\mathbf{i},\mathbf{j}-\mathbf{a}} + \Delta_{\mathbf{i}}^{x-}\delta_{\mathbf{i},\mathbf{j}+\mathbf{a}} + (\Delta_{\mathbf{i}}^{y+}\exp[i\mathbf{k}a] + \Delta_{\mathbf{i}}^{y-}\exp[-i\mathbf{k}a])\delta_{\mathbf{i},\mathbf{j}}].$$

Here

$$t_{\mathbf{ij}\sigma} = \begin{cases} t_{F\sigma} & \mathbf{i},\mathbf{j} \in \mathrm{F\ side}, \\ t_S & \mathbf{i},\mathbf{j} \in \mathrm{S\ side}, \\ t_T & \mathbf{i} \in \mathrm{F\ side},\ \mathbf{j} \in \mathrm{S\ side\ (interface)} \end{cases}$$

and

$$V_{\mathbf{ij}} = \begin{cases} 0 & \mathbf{i},\mathbf{j} \in \mathrm{F\ side}, \\ V_S & \mathbf{i},\mathbf{j} \in \mathrm{S\ side}, \\ 0 & \mathbf{i} \in \mathrm{F\ side},\ \mathbf{j} \in \mathrm{S\ side\ (interface)}. \end{cases}$$

We assume that the probability of charge transfer at the interface is independent of the spin orientation and does not include any spin scattering effect. Finally, the exchange field $h_{\mathbf{i}}$ is equal to h_F if the site $\mathbf{i}$ belongs to the F subsystem, and is zero otherwise.

To determine the self-consistent solutions of the problem, one diagonalizes the mean-field Hamiltonian introducing a unitary transformation in the particle-hole space for the electron operators, defined in terms of the components $[u_{\mathbf{i}n}(\mathbf{k}), v_{\mathbf{i}n}(\mathbf{k})]$ of the n-th eigenvector:

$$\alpha_n(\mathbf{k}) = \sum_i [u_{\mathbf{i}n}(\mathbf{k}) c_{\mathbf{i}\uparrow}(\mathbf{k}) + v_{\mathbf{i}n}(\mathbf{k}) c_{\mathbf{i}\downarrow}^{\dagger}(-\mathbf{k})].$$

Such transformation diagonalizes the Hamiltonian H_{MFA}, providing the solution of the Bogoliubov-de Gennes equations

$$\sum_{\mathbf{j}} \hat{h}_{\mathbf{ij}}(\mathbf{k}) \begin{bmatrix} u_{\mathbf{j}n}(\mathbf{k}) \\ v_{\mathbf{j}n}(\mathbf{k}) \end{bmatrix} = E_n(\mathbf{k}) \begin{bmatrix} u_{\mathbf{i}n}(\mathbf{k}) \\ v_{\mathbf{i}n}(\mathbf{k}) \end{bmatrix} \tag{5}$$

for each value of the momentum $\mathbf{k}$. In terms of the eigenvectors components $[u_{\mathbf{i}n}(\mathbf{k}), v_{\mathbf{i}n}(\mathbf{k})]$ and the eigenvalues $E_n(\mathbf{k})$, the order parameters are given by

$$\Delta_{\mathbf{i}}^{x\pm} = \frac{1}{N_y} \sum_{\mathbf{k},n} u_{\mathbf{i}n}(\mathbf{k}) v_{\mathbf{i}\pm\mathbf{a},n}^{*}(\mathbf{k}) \{1 - f[E_n(\mathbf{k})]\},$$

$$\Delta_{\mathbf{i}}^{y\pm} = \frac{1}{N_y} \sum_{\mathbf{k},n} u_{\mathbf{i}n}(\mathbf{k}) v_{\mathbf{i},n}^{*}(\mathbf{k}) \{1 - f[E_n(\mathbf{k})]\} \exp[\mp i\mathbf{k}a],$$

$$n_{\mathbf{i}\uparrow} = \frac{1}{N_y} \sum_{\mathbf{k},n} |u_{\mathbf{i}n}(\mathbf{k})|^2 f[E_n(\mathbf{k})],$$

$$n_{\mathbf{i}\downarrow} = \frac{1}{N_y} \sum_{\mathbf{k},n} |v_{\mathbf{i}n}(\mathbf{k})|^2 \{1 - f[E_n(\mathbf{k})]\},$$

where $f[E_n(\mathbf{k})]$ is the Fermi distribution function for electrons with eigenenergy $E_n(\mathbf{k})$. Hereafter, we follow a standard procedure for the solution of the above self-consistent equations: (i) start with an initial set of values for the order parameters, (ii) solve the Bogoliubov-de Gennes equations, and (iii) redetermine the amplitudes for the order parameters and proceed by iteration until the required accuracy is reached. For the different cases upon examination, we have analyzed different starting points in the space of the order parameters and when more than one solution is obtained, a criterion of minimum free energy is used to select the most stable one. The numerical simulation has been performed on a bilayer system with size $L_x = L_y = 120$, with the position of the interface corresponding to the coordinate $x = 60$ (all the lengths are in units of the interatomic lattice spacing a). We have also verified that for larger values of the size of the system, the results obtained here remain qualitatively the same.

III. PROXIMITY EFFECTS IN THE F/US BILAYER

As already pointed out in Sec. II, we are interested in the analysis of the proximity effect between an unconventional superconductor and a ferromagnet with a magnetization due to a constant exchange field ($h_F = h$) and/or to a bandwidth asymmetry for electrons with opposite spins ($t_{F\uparrow} \neq t_{F\downarrow}$). The analysis of the proximity involving a Stoner-type ferromagnet has shown in the cases of chiral p-wave and d-wave order parameters that there are other components near the interface that can be induced in a symmetry channel that is different from the one of the bulk region.[36,35] Moreover, for a time-reversal broken-symmetry state a spontaneous current can flow along the interface where the OP has a variation in space.[35] Here, we rather concentrate on a peculiar aspect concerning the character of the induced components at the interface that has not been considered so far. Indeed, we show that the presence of a finite magnetization with a nonzero average $m_{\mathbf{i}}$, and at the same time both $\langle n_{\mathbf{i}\uparrow}\rangle \neq 0$ and $\langle n_{\mathbf{i}\downarrow}\rangle \neq 0$, induces interface components with a symmetry different from that of the bulk domain, which propagate in the ferromagnetic part with a significantly long range of oscillation.

We stress that in the case of triplet bulk symmetry the origin of the induced singlet OPs at the interface is not due to the suppression of the dominant p-wave component, since near the surface of a triplet superconductor faced to vacuum the singlet ones are not present.[37] Rather, it is the specific occurrence of a proximity state with $\langle n_{\mathbf{i}\uparrow}\rangle \neq \langle n_{\mathbf{i}\downarrow}\rangle$ that yields an interface state with a mixed singlet-triplet configuration. Indeed, due to the spin rotational breaking field, the probability of pairing $|\Delta(\mathbf{k}\uparrow, -\mathbf{k}\downarrow)|^2$ for two electrons with wave vectors and spins $(\mathbf{k},\uparrow)$ and $(-\mathbf{k},\downarrow)$ is different from the prob-

ability $|\Delta(\mathbf{k}\downarrow,-\mathbf{k}\uparrow)|^2$ of having an electron pair where the two spins are reversed. Therefore singlet superconductivity, which is characterized by a spin OP such that $\Delta(\uparrow,\downarrow)=-\Delta(\downarrow,\uparrow)$, has to come mixed with a triplet component for which $\Delta(\uparrow,\downarrow)=\Delta(\downarrow,\uparrow)$ and vice versa. Such symmetry requirement holds in a specular way also in the case where one has singlet bulk symmetry and triplet interface components and links together the proximity leaking of the Cooper pairs in the singlet and triplet channel within the F side.

A. F/US bilayer with chiral p-wave symmetry

We start by selecting a set of parameters and an electron density such that the ground state has a p-wave character with broken parity and broken time reversal symmetry $(p_x \pm ip_y)$. Previous studies on the extended Hubbard model[38,39] have shown that a $d_{x^2-y^2}$-wave superconducting state is stabilized near half filling $(\mu \sim 0)$, while an extended s wave appears at high (and low) densities for $|\mu|$ falling in a range going approximately from $2.5t$ to $4t$. In the region between d- and s-wave states, the spin triplet $p_x \pm ip_y$ occurs. In this case, the states p_x+ip_y and p_x-ip_y are degenerate but unequal as they transform into each other by applying the parity and the time-reversal symmetry operation. Concerning the ferromagnetic side of the bilayer, we use the exchange field h and the bandwidth asymmetry ratio $t_{F\downarrow}/t_{F\uparrow}$ as tuning control parameters, keeping the local Coulomb repulsion below the Stoner threshold. This choice is motivated by the necessity of having ferromagnetic configurations with nonvanishing densities for both spin-up and spin-down electrons. In addition, the presence of the mechanism of mass split exchange allows to explore how the proximity is modified by the change in shape of the Fermi surfaces for electrons with opposite spins.

Hence, we will discuss the outcome of the proximity within the F/US bilayer assuming a value of the chemical potential equal to $\mu=-1.6$, with $U_F=2$, $V_F=0$ for the F side and $U_S=1.5$, $V_S=-2.5$ for the US side; all the energies being expressed in units of $t_{S\uparrow}=t_{S\downarrow}=t_{F\uparrow}=1$. Furthermore, in the following the tunneling matrix element is kept fixed and chosen equal to $t_T=1$. For these values of the microscopic parameters, the US side exhibits a bulk OP with triplet p_x+ip_y symmetry, whereas the induced components in the singlet channel at the interface show a different behavior depending on the strength of the magnetic exchange couplings. Our main findings are summarized in the phase diagram reported in Fig. 1 as a function of the exchange field h and of the bandwidth asymmetry ratio. Here we individuate two regions, one characterized by short-range (SR) -induced components at the interface, essentially coinciding with the half-metallic phase where $n_{F\downarrow} \simeq 0$, and the other one characterized by a longer leaking distance in the F side and an oscillating character [oscillating long-range (LROS)]. In the SR region s- and d-wave components exhibit a partial penetration into the F system with a strongly damped character, while in the LROS one they propagate over the whole length of the F side, with a weakly damped oscillating character. The separation between the two regions is of course not sharp, in the sense that no real transition occurs at the boundary. Rather,

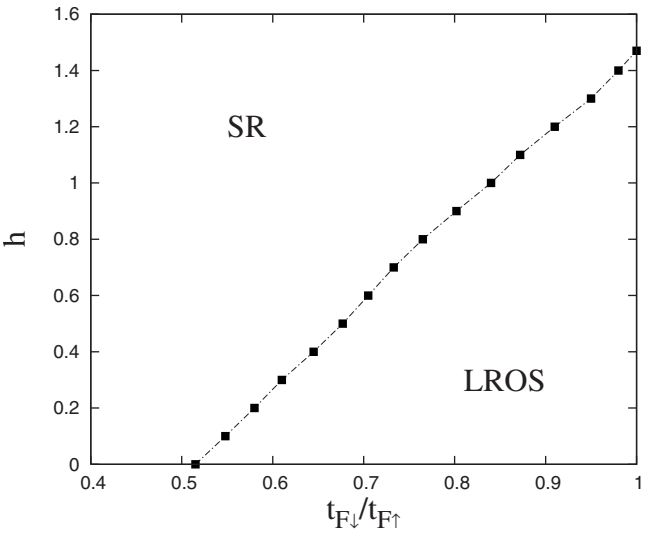

FIG. 1. Ground-state diagram for the F/US bilayer with p-wave symmetry in terms of the exchange field h and the mass split asymmetry ratio $t_{F\downarrow}/t_{F\uparrow}$. Here SR and LROS stand for short range and long range oscillating proximity of the induced OP components at the interface, respectively. The SR region essentially coincides with the half-metal phase. The parameter values are $U_F=2$, $V_F=0$ for the F side and $U_S=1.5$, $V_S=-2.5$ for the S side, with $\mu=-1.6$.

they are separated by a crossover line corresponding to a smooth changeover from the long-range oscillating behavior to the short-range one as the spin polarization increases. This crossover line has been drawn looking at the values of h and $t_{F\downarrow}/t_{F\uparrow}$ for which the amplitude of the order parameter oscillations fully decays over a distance from the interface (located at $x/a=L/2$) corresponding to $x/a \simeq L/4$.

As discussed previously, for the case under consideration of bulk chiral p-wave symmetry the presence of a finite magnetization in the F side leads to a pairing amplitude in the s- and d-wave channel at the interface. Hence, by suitably tuning the amplitude of the exchange field and that of the hopping asymmetry ratio, it is possible to control the leaking distance of the induced pairs and the profile of the pairing amplitude. Explicit evidence of the existence of the two regimes appearing in the phase diagram of Fig. 1 is provided in Fig. 2, where we show the spatial dependence of the singlet and triplet components in the case of ferromagnetism generated solely by the spin mass asymmetry mechanism. We observe for each component slowly damped long-range oscillations with amplitude and period gradually reducing to zero as the ratio $t_{F\downarrow}/t_{F\uparrow}$ is decreased. The propagation becomes fully inhibited when this ratio reaches a value (for the parameter chosen here approximately equal to 0.4) leading the ferromagnetic layer in the half-metallic regime with no minority carriers. We also notice that the imaginary parts of both the s- and the d-wave components, not shown here for brevity, are appreciable at the interface but decay very quickly as one moves away from it, in a way which is essentially insensitive to the degree of magnetization in the F layer.

Similar conclusions can be drawn in the case when the ferromagnetism is generated by the presence of an exchange field. As one can see from Fig. 3, again we have a tendency

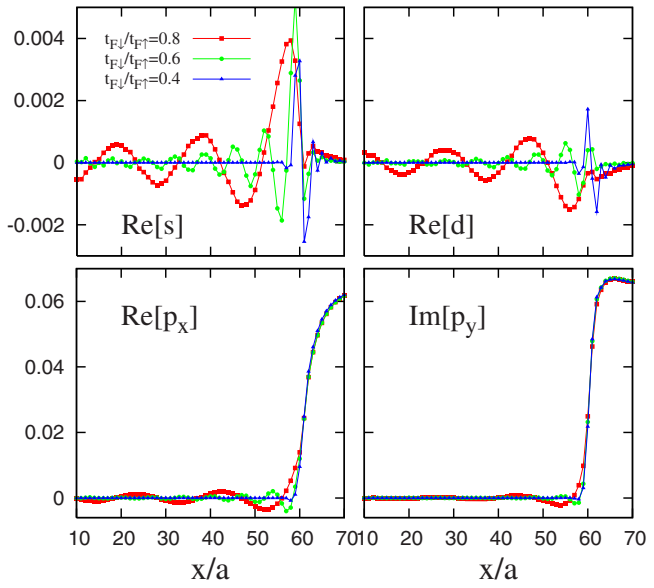

FIG. 2. (Color online) Spatial variation of the superconducting OPs for the F/US bilayer with chiral p-wave symmetry for $h=0$ and three different values of hopping asymmetry ratio $t_{F\downarrow}/t_{F\uparrow}$. The upper panels show the real part of the singlet extended s- and d-wave OPs. The lower panels show the real part of the p_x-wave OP and the imaginary part of the p_y-wave OP, respectively.

to the suppression of the oscillating propagation in the F side as the field is increased up to values leading to $n_{F\downarrow} \simeq 0$. To further clarify these issues, we have reported in Fig. 4 the behavior of $n_{F\uparrow}$ and $n_{F\downarrow}$ in proximity of the interface ($x/a=58$) as the exchange field or the hopping ratio are varied. We see that the increase in h leads to an increase in $n_{F\uparrow}$ and a decrease in $n_{F\downarrow}$, as a consequence of the relative shift of the two bands, while the decrease in $t_{F\downarrow}/t_{F\uparrow}$ leads to a similar effect on $n_{F\downarrow}$, now associated with the narrowing of the down-spin bandwidth, with $n_{F\uparrow}$ remaining approximately constant, as expected.

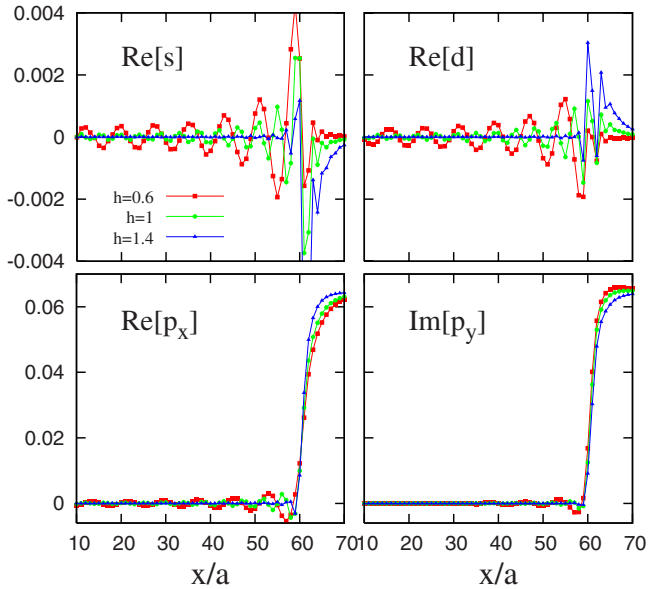

FIG. 3. (Color online) Same as in Fig. 2 for $t_{F\downarrow}/t_{F\uparrow}=1$ and three different values of the exchange field h.

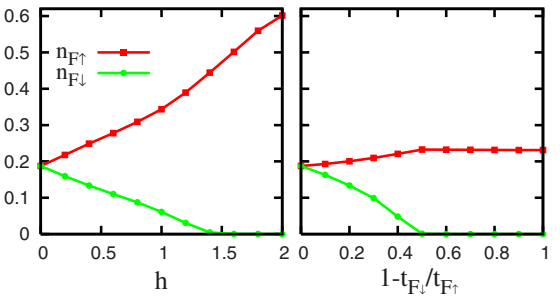

FIG. 4. (Color online) Variation of the electron densities in the ferromagnetic layer at the site $x/a=58$ for a F/US bilayer with the p-wave symmetry. The case where $h \neq 0$ and $t_{F\downarrow}/t_{F\uparrow}=1$ is reported in the left panel, while the reversed case where $h=0$ and $t_{F\downarrow}/t_{F\uparrow} \neq 1$ is reported in the right panel.

The establishment of the half-metallic regime also determines the position of the boundary between the SR and the LROS regime characterizing the phase diagram in Fig. 1. Indeed, as in the cases previously discussed, where only one mechanism was effective, the crossover takes place at values of $t_{F\downarrow}/t_{F\uparrow}$ and h for which the density of the minority electrons tends to zero and only one type of carrier is polarized and contributes to the transport. This amounts to say that at the boundary the Fermi surface of the minority spin carriers shrinks to zero, this being determined by the condition that for no values of $\mathbf{k}$ the energy spectrum $\varepsilon_{\mathbf{k}\downarrow}$ becomes equal to the renormalized chemical potential $\bar{\mu}=\mu-U_F\langle n_{\mathbf{i},\uparrow}\rangle+h$. This evidently happens when $t_{F\downarrow}/t_{F\uparrow}$ and h are such that the equation

$$-2t_{F\downarrow}[\cos(k_x a)+\cos(k_y a)]-\mu+U_F\langle n_{\mathbf{i},\uparrow}\rangle+h=0 \quad (6)$$

admits no solution.

Few more aspects are worth to be pointed about the profile of the induced singlet components in the LROS regime. The period of oscillation is inversely proportional to the strength of $t_{F\downarrow}/t_{F\uparrow}$ and to h, and it generally shrinks as the density of minority spins decreases to zero. Moreover, the fact that no qualitative changes are found when comparing the effect of the exchange field and that of the spin bandwidth asymmetry only holds provided that the sign of the hopping amplitude for the two spin species is the same. Actually, we have checked that the LROS behavior is destroyed by the presence in the F side of a mixed configuration, where the Fermi surface is electronlike for one spin species and holelike for the other one. Considering that in the S layer the hopping amplitude is the same for up and down spins, in this situation we have a Fermi surface mismatch between the F and the S side active in a single spin channel, which nonetheless can lead to a significant pair-breaking effect and a corresponding severe damping of the order parameter. This is confirmed by the fact that, even in the presence of a nonvanishing density of the electrons in both the majority and the minority spin channel, the induced pairing amplitude in the singlet, as well as in the triplet channel, does not exhibit any long-range oscillating profile, this reflecting the drastic reduction of the penetration of the Cooper pairs into the ferromagnetic region.

Let us also point out that within the mean-field decoupling of the attractive nearest-neighbor term, we have not considered the possibility of an order parameter corresponding to equal spin pairing (ESP). The main motivation for this choice resides in the fact that no possibility of having magnetically ordered states in the S layer has been considered. Nonetheless, superconducting triplet components with nonvanishing projection along the quantization axis could come into play at the interface when the half-metal regime is reached.

The consideration of ESP components is of interest also in connection with the possible generation of odd-frequency triplet pairing correlations.[40] In our approach we confined ourselves to the case of time-independent order parameters, this implying that the dominant superconducting components must necessarily be of the even-frequency type. Nonetheless, we believe that within a suitable generalization of our approach, odd-frequency components may develop at the interface as a consequence of our choice of a pairing potential effective between different (nearest-neighbor) sites. Indeed, in the case of strong spin polarization this choice may lead to the formation in proximity of the interface of triplet components with $S_z = \pm 1$, which can be associated with odd-frequency pair amplitudes. This can happen with no need of a rotation in the magnetization at the ferromagnet/superconductor interface[41] or of different orientations of the magnetization in the two ferromagnetic layers of ferromagnet/superconductor/ferromagnet trilayer structures,[42,43] which on the contrary are necessary when a standard on-site attractive potential is assumed for the S side.

B. *F*/*US* bilayer with *d*-wave symmetry

In the same spirit of the investigation performed previously for the triplet case, we analyze the proximity behavior in the bilayer F/US in the case of an unconventional superconductor marked by a bulk OP component with $d_{x^2-y^2}$ symmetry. Here the parameters to get superconductivity in the d-wave channel are the same as those chosen for the triplet case, with the exception of a slightly lower absolute value of the intersite attractive coupling ($V_S = -1.5$) and a value of the chemical potential ($\mu = -0.2$) leading to a higher total electron density. All the other parameters, i.e., the interface hopping amplitude t_T and the parameters characteristic of the ferromagnetic layer, are left unchanged.

The proximity-induced subdominant components now develop in the p_x, p_y, and extended s-wave channel, with the most stable solutions being the ones without any time reversal symmetry breaking. The results obtained in this case, concerning the interplay between the bulk symmetry and the one of the induced components, exhibit some kind of duality when compared to those previously found for a bulk chiral p-wave symmetry. In this case too, we start by presenting the ground-state phase diagram for the induced OP components at the interface (see Fig. 5), distinguishing among a SR penetration region and an LROS one (see Fig. 6 for the case $h = 0$, $t_{F\downarrow}/t_{F\uparrow} \neq 1$, and Fig. 7 for the case $h \neq 0$, $t_{F\downarrow}/t_{F\uparrow} = 1$).

As in Fig. 1, the crossover line separating the SR and the LROS shows an almost linear dependence of $t_{F\downarrow}/t_{F\uparrow}$ versus h, but now the half-metallic phase does not coincide anymore with the SR region. In this circumstance too, it is possible to understand the origin of the oscillating behavior from the behavior of the electron densities $n_{F\uparrow}$ and $n_{F\downarrow}$ in proximity of the interface in the ferromagnetic layer. Indeed, from Fig. 8 we can see that the changeover from the LROS to the SR regime is generally accompanied by a reduction to zero

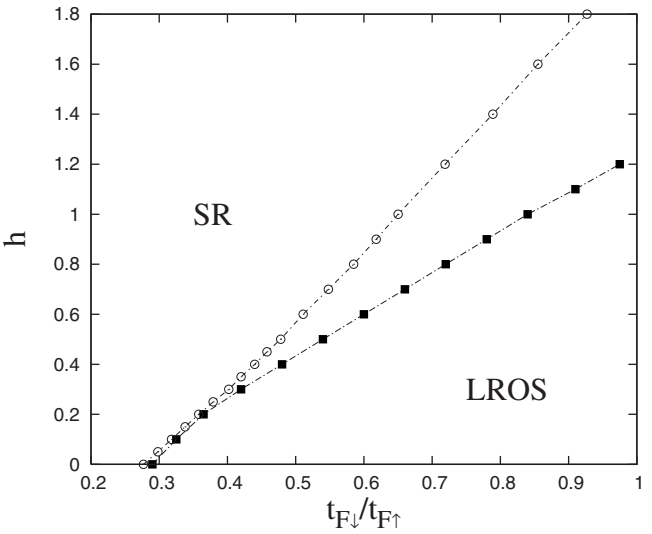

FIG. 5. Ground state phase diagram for the F/US bilayer with d-wave symmetry in terms of the exchange field h and the mass split asymmetry ratio $t_{F\downarrow}/t_{F\uparrow}$. As for Fig. 1, full squares separate the regimes characterized by SR and LROS induced OP components at the interface. The region above the open circles corresponds to the half-metallic phase. The parameters are the same as in Fig. 1, except for $V_S = -1.5$ and $\mu = -0.2$.

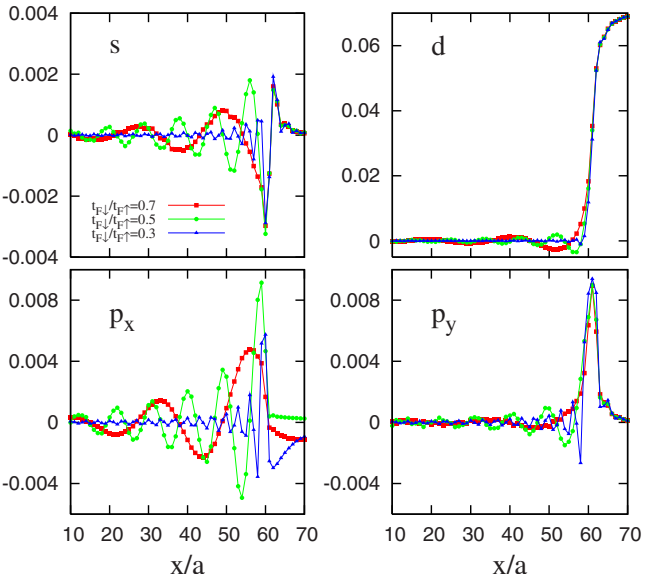

FIG. 6. (Color online) Spatial variation of the superconducting OPs for the F/US bilayer with d-wave symmetry for $h = 0$ and three different values of hopping asymmetry ratio $t_{F\downarrow}/t_{F\uparrow}$. The singlet extended s- and d-wave OPs are shown in the upper panels, while the p_x- and the p_y-wave OPs are shown in the lower ones (all the superconducting components here are real).

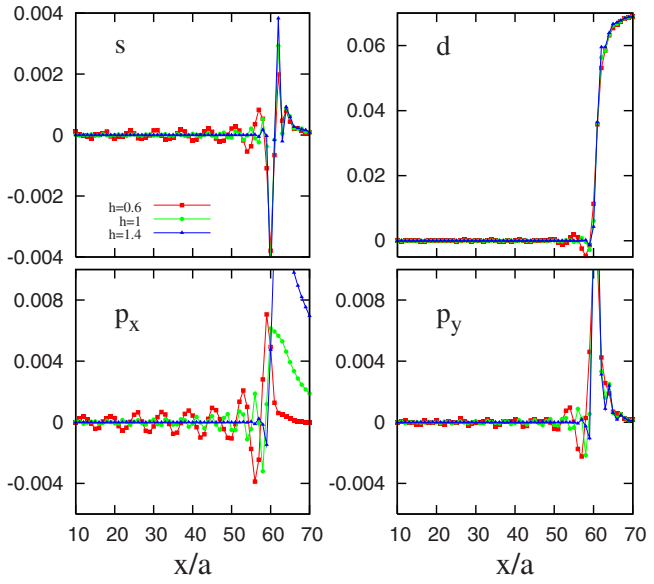

FIG. 7. (Color online) Same as in Fig. 6 for $t_{F\downarrow}/t_{F\uparrow}=1$ and three different values of the exchange field h.

of the minority spin density, implying the transition to a half-metallic regime. As for the previous case, an estimation of the crossover values $t^*_{F\downarrow}/t^*_{F\uparrow}$ and h^* can be obtained by solving Eq. (6) and extracting the exchange amplitudes, where the associated Fermi surface shrinks to zero. Looking at the previous expression, one can indicate in the unequal amplitude of the chemical potential for the p- and d-wave symmetry, the difference in the threshold amplitude for setting the SR regime.

IV. DENSITY OF STATES AT THE INTERFACE

To further characterize the proximity effect for the bilayer system under examination, we have considered the modification of the density of states (DOS) at the interface, with the purpose of comparing the features due to the different spin polarizing mechanisms. The variation of the local density of states at the interface between a superconductor and a normal metal or a ferromagnet has been widely discussed in literature upon different microscopic conditions. These studies have been performed in the diffusive,[4,44,45] as well as in the clean limit[46] within different schemes of computations and

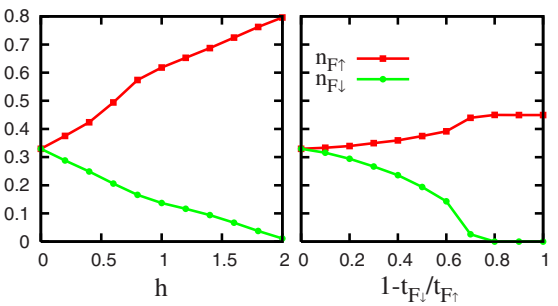

FIG. 8. (Color online) Same as in Fig. 4 in the case of a F/US bilayer with d-wave symmetry.

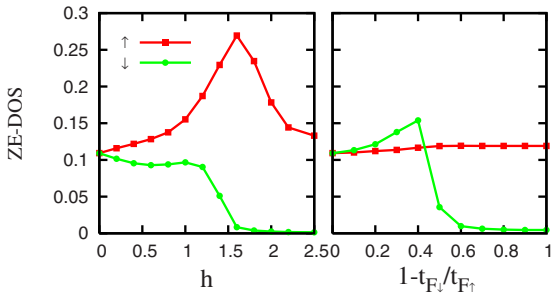

FIG. 9. (Color online) Representative evolution of the zero-energy density of states (ZEDOS) in the ferromagnetic side for the minority and the majority electron spin density at the site $x/a=58$ versus the spin-exchange field (left panel) and the spin-hopping asymmetry (right panel). The parameter values are the same as those leading to the triplet phase discussed in Sec. III A.

accounting for a conventional or unconventional pairing potential, respectively.

Hereafter, our analysis is focusing on few special distinctive aspects of this issue, starting from the consideration of an unconventional superconductor with triplet p-wave chiral pairing. The investigation takes into account the energy dependence of the density of states around the Fermi level in the case of a magnetic polarization due to either spin-exchange field or spin-dependent mass. We shall show that the differences emerging in the ferromagnetic side in the behavior of the zero-energy density of states (ZEDOS) for majority and minority spin electrons influence the modification of the DOS in the superconductor when the effective spin exchange or the spin-dependent hopping asymmetry are varied. Moreover, as in the previous Sections, we concentrate on a specific interface configuration with (100) direction, in the case of high barrier transparency.

In Fig. 9 we report the changes of the ZEDOS induced by variations of the spin-exchange field and the spin-dependent hopping asymmetry at a site position in proximity of the interface within the ferromagnetic side. The curves here refer to the same parameter choice adopted in the discussion of the bulk triplet case. Some indicative information can be extracted from Fig. 9. The behavior of the ZEDOS reflects the DOS curvature for the ferromagnetic subsystem as given by the two different ways of generating spin polarization via h or $t_{F\downarrow}/t_{F\uparrow}$. Indeed, the variation of the spin exchange field leads to a relative energy shift of the spin majority DOS with respect to the spin minority one. This in turn implies a shift of the chemical potential within the majority DOS lower band. Since we are considering a nearest neighbor hopping connectivity on a square lattice in two dimensions, the DOS exhibits a single peak associated with an extremal point for the energy dispersion (van Hove singularity). Hence, the ZEDOS of the majority spin will go through a maximum at about $h\sim 1.6$ before getting down to a value that is comparable with that of the normal zero-field configuration. On the other hand, the ZEDOS for the minority spin is monotonically decreasing until it goes to zero at the transition to the half-metallic state for a critical exchange amplitude given by $h_{HM}\sim 2.5$.

When considering the ferromagnetic configuration generated by a spin-dependent hopping asymmetry, it is the ratio

between the spin bandwidths (or the renormalized masses) to be varied. This corresponds to an effective reduction of the minority spin bandwidth with respect to the majority one, accompanied by an increase in the intensity arising to keep the total spectral weight conserved. As discussed in the Sec. I this type of ferromagnetism originates as a net gain in the kinetic energy for the majority spin component. As a consequence of this microscopic modification of the hopping amplitude, the ZEDOS for the majority spin stays almost constant while the one for the minority spin follows the DOS curvature reaching a maximum at $1-t_{F\downarrow}/t_{F\uparrow}\sim 0.4$ and then becoming quickly suppressed when approaching the half-metallic limit around $1-t_{F\downarrow}/t_{F\uparrow}\sim 0.7$. Indeed, below this value the narrowing of the spin down band makes the DOS entirely develop at energies above the chemical potential, in such a way to give $n_{\downarrow}\simeq 0$.

In summary, the behavior of the ZEDOS is highly nontrivial as the amplitude of the spin polarizing interactions is changed, as a consequence of the specific form of the two-dimensional normal state DOS for nearest-neighbor hopping on a square lattice. Two distinct behaviors for the majority and the minority spin components can be extracted when the spin-exchange field or the spin-dependent mass mechanism are considered. Such differences are of guide to interpret the manifestation of the ferromagnetic correlations in the proximity involving different DOS spin channels. Let us also notice that a similar behavior as the one shown in Fig. 9 is found in the *d*-wave case, the only difference consisting in a shift of the curves toward lower values of h and $1-t_{F\downarrow}/t_{F\uparrow}$, as a consequence of the closer proximity of the chemical potential to the van Hove singularity.

As far as computational aspects are concerned, the site-dependent DOS is evaluated at the end of the self-consistent procedure for the determination of the superconducting order parameters and the magnetization profile. In terms of the eigenvectors components $[u_{in}(\mathbf{k}),v_{in}(\mathbf{k})]$ and the corresponding eigenvalues $E_n(k)$, the local DOS for spin component at the i-th site $(i\equiv x/a)$ is given by:

$$N_{i\uparrow}(\omega)=\frac{1}{N_y}\sum_{k,n}|u_{in}(k)|^2\delta[\omega-E_n(k)],$$

$$N_{i\downarrow}(\omega)=\frac{1}{N_y}\sum_{k,n}|v_{in}(k)|^2\delta[\omega+E_n(k)].$$

In the following subsections, the results will be presented by normalizing the DOS for the general $F-S$ case to the one for the nonsuperconducting $(F-N)$ bilayer configuration evaluated at zero strength of the pairing coupling. Thus, all the variations with respect to the unit amplitude are a consequence of the interplay between the pair formation and the spin imbalance in the ferromagnetic side of the junction. For convenience, we will also scale the energies by using the value of the gap Δ_0 obtained well inside the superconductor, i.e., where the pairing amplitude is not influenced by the interface, also fixing the chemical potential at $\omega=0$.

We point out that the experimental detection of a spin-resolved DOS can be performed via scanning tunneling spectroscopy (STS) by using a tip made of a half metal (such as, for instance, CrO_2) allowing for the transfer of only one type of carrier. This kind of technique has already been used in the past to directly probe the spectral density for majority and minority carriers in magnetic systems such as chromium[47] or manganese[48] thin films. Tip designs and modes of operation for spin-polarized STS have been recently reviewed in Ref. 49, where the analysis has also been referred to the case of planar tunnel junctions made of different electrode materials, such as superconductors, optically excited GaAs, and ferromagnets.

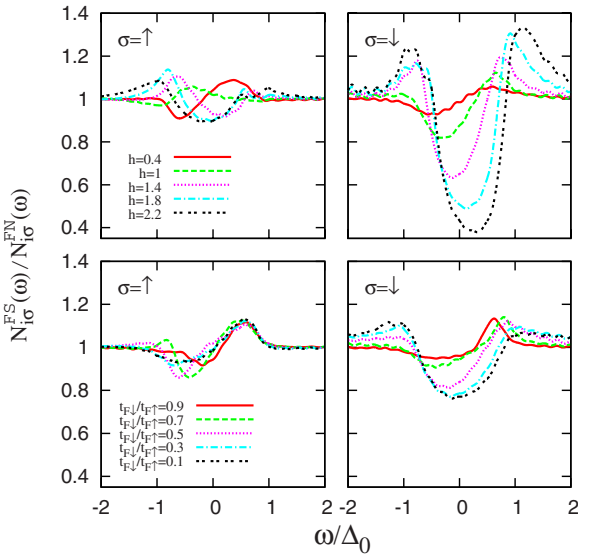

FIG. 10. (Color online) Normalized DOS at the interface $(i=x/a=L/2)$ in the case of chiral p-wave symmetry for majority $(\uparrow)$ and minority $(\downarrow)$ spin components for $t_{F\downarrow}/t_{F\uparrow}=0$ and several values of the exchange field h (upper panels), and for $h=0$ and several values of the asymmetry hopping ratio $t_{F\downarrow}/t_{F\uparrow}$ (lower panels).

A. F/*p*-wave bilayer

In Fig. 10 we compare the effects induced by variations of the spin field and the mass asymmetry on the density of states evaluated at the interface site position (i.e., $i=x/a=L/2$). This choice is motivated by the fact that the interface behavior contains some of the main distinctive features characterizing the two mechanisms. The strategy we follow is to consider separately the behavior of the DOS for the two spin polarizing mechanisms and then to analyze the main differences between them. To start with, we discuss the DOS structure for each spin polarization as a function of h. In the upper panels of Fig. 10 we report the behavior of the DOS for the up- and down-spin channel versus the exchange field amplitude. From a quantitative point of view, no significant variations can be observed for the majority spin band, although a reversal of the DOS profile occurs when the field amplitude is raised above the value corresponding to the ZEDOS maximum (see Fig. 9). On the other hand, the effects are very pronounced in the minority spin channel because minority spin electrons have a high probability to pair up with the electrons coming from the majority spin band within the ferromagnet. Such paired configurations are mainly re-

sponsible for the DOS modification inside the gap in the down spin channel. For the majority spin channel, the spectral weight is weakly modified except for the change induced by the residual minority electron spin density in the ferromagnet.

Going more into detail, one can notice that for the minority spin channel the normalized DOS profile exhibits (i) a dip/peak structure at energies below/above zero for low-spin field, (ii) a well-defined gaplike structure deepening more and more as the half-metallic limit is approached, accompanied by the formation of pseudo-quasiparticle coherent peaks at energies $\pm\Delta_0$.

The dip/peak positions are at energies of the order of $\Delta_0/2$ but they are not symmetric. They are gradually shifted toward higher frequencies until the value $h\sim 1.7$, corresponding to the turning point of the ZEDOS in the minority spin channel, is reached. Above this threshold, an enhancement of the spectral weight occurs at energies corresponding to pair breaking and quasiparticles formation. An interesting aspect is represented by the hardening of the gap in the minority spin component as the exchange field is increased. This result seems counterintuitive if one considers that approaching the half-metallic limit the decrease in the minority carrier density should lead to a suppression of the pairing amplitude. However, as a stronger and stronger unbalance between the two spin species is created, the corresponding increase in the singlet component at the interface (which is absent for $n_\uparrow=n_\downarrow$) becomes responsible for the deepening of the gap in the minority spin channel. This can easily be understood considering that the reduction of the down spin component in the ferromagnetic side tends to induce an order parameter, due to the pairing of up spins in the F side with down spins coming from the S side, that is built via a superposition of singlet and triplet pairing amplitudes. This process is also favored by the increase in the majority spin carriers seen as one moves toward the half-metallic regime (see Figs. 4 and 8).

Going to the differences found in the DOS when the two mechanisms for ferromagnetism are considered, we notice that they can be ascribed to the specific peculiarities at the interface shown by the x and y components (perpendicular and parallel to the interface, respectively) of the chiral p-wave superconducting order parameter considered here. These two components, combined in the form p_x+ip_y, are affected to a different extent by the two spin-polarizing mechanisms as one approaches the half-metallic limit. This is particularly evident in the behavior of the correlation length associated with the distance from the interface of the point where the pairing amplitude reaches its bulk value. While this distance is sensible to the strength of the exchange field, on the contrary it stays constant as decreasing values of the mass asymmetry ratio are considered (see lower panels of Fig. 3 and Fig. 2, respectively).

B. F/*d*-wave bilayer

Similar considerations can also be made for the case of a **F**/*d*-wave bilayer. Again a crucial role is played by the way the DOS for up- and down-spin electrons in proximity of the

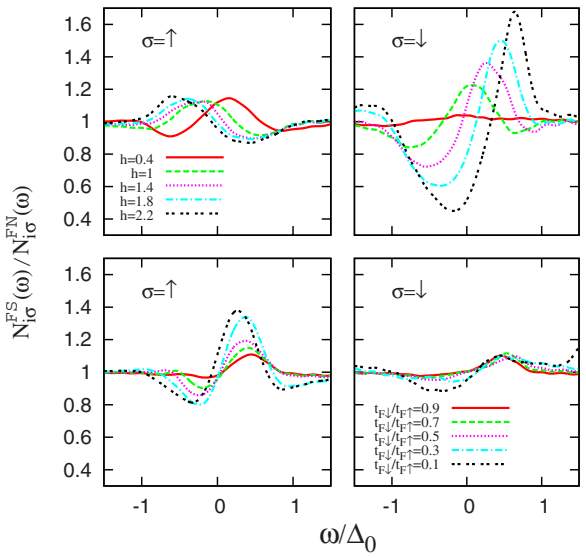

FIG. 11. (Color online) Same as in Fig. 10 in the case of d-wave symmetry.

Fermi level is affected by variations of the exchange field or variations of the mass asymmetry ratio. The behavior is similar to the one showed in Fig. 9, except that in the case of field variations the maximum for the majority spin DOS at zero energy is reached at a much lower value of h (approximately equal to 0.6), as a consequence of the fact that the d-wave phase develops at higher electron densities with respect to the p-wave case, corresponding to values of the chemical potential much closer to the van Hove singularity.

The behavior of the DOS for up and down spin as the exchange field is varied is reported in the upper panels of Fig. 11. The results are not very different from the ones obtained in the case of p-wave symmetry. The DOS for majority (up) spins exhibits an even more well-defined dip/peak structure at low fields that gets reversed into a peak/dip one as the relative band shift due to the increase in h makes the chemical potential cross the van Hove singularity. The inversion point coincides with the value $h=0.6$ of the field at which the up-spin zero-energy DOS takes its maximum value. At the same time, the amplitude of the structures stays approximately constant as the field is varied. On the other hand, as for the p-wave case, the increase in the field leads to a substantial deepening of the gaplike structure in the DOS for minority spin-down electrons. This is again due to the increase in the majority spin electron density as the half-metallic regime is approached, together with the corresponding strengthening of the triplet components of the order parameter. However, differently from what happens for the p-wave symmetry, the DOS for minority down-spin electrons does not exhibit a symmetrically developed gaplike structure with quasiparticle peaks at $\pm\Delta_0$ even for values of the field well above the one ($\sim$1.8) at which the half-metallic regime is reached. This behavior can be understood in terms of the different behavior characterizing the triplet components in the two cases of Stoner-like and mass spin asymmetry mechanism for ferromagnetism considered here. Actually, while p_x and p_y components appreciably increase when the value of the exchange field is raised, on the contrary they

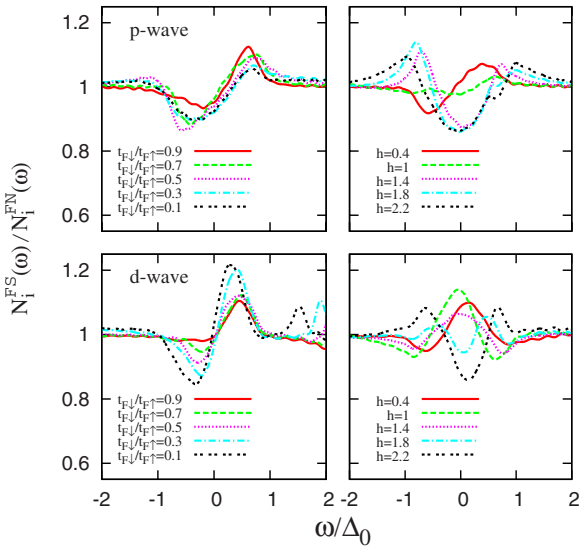

FIG. 12. (Color online) Normalized total DOS at the interface $(i=x/a=L/2)$ in the cases of chiral p-wave (upper panels) and d-wave symmetry (lower panels). The curves in the left and in the right panels refer to the case of ferromagnetism generated by the spin bandwidth asymmetry and by the Stoner-like mechanism, respectively.

stay approximately constant when lower and lower values of the mass asymmetry ratio are considered.

We conclude this section by showing in Fig. 12 the behavior of the total DOS

$$N_i(\omega) = N_{i\uparrow}(\omega) + N_{i\downarrow}(\omega)$$

evaluated at the interface $(i=x/a=L/2)$ and normalized to its normal state value. We can clearly see that there is a substantial difference in the results for the total DOS obtained when the two kinds of mechanism for ferromagnetism are considered. In the case of spin bandwidth asymmetry, the DOS is asymmetric with respect to zero energy, regardless of the value of $t_{F\downarrow}/t_{F\uparrow}$ for both p- and d-wave pairing. On the contrary, in the case of ferromagnetism due to the presence of an exchange field h, the total DOS exhibit peaks which are gradually shifted in position as h is varied, with the formation of a gap symmetrically developing around zero energy when the half-metallic regime is reached. This occurs essentially in the same way for both kinds of symmetry, the main difference between them residing in the presence in the d-wave case of a zero-bias maximum at intermediate values of h, which is absent in the p-wave case.

V. CONCLUSIONS

We have investigated the behavior of a bilayer junction made of an unconventional superconductor and an itinerant ferromagnet, separately considering for the former the two cases of chiral p-wave and d-wave symmetry, and for the latter two distinct mechanisms for the generation of spin unbalance, that is, (i) a Stoner-like one originated by the presence of a constant exchange field, and (ii) a mass asymmetry one generated by a narrowing of the bandwidth of the minority spin carriers with respect to the majority ones. The rich phenomenology of this kind of system is of particular interest because the interface properties of d- and p-wave superconductors are quite different from those exhibited by conventional isotropic s-wave ones, due to the nontrivial angular structure of the corresponding pair wave functions. In particular, as soon as a finite magnetization appears, very specific effects take place as a consequence of the propagation in the ferromagnetic layer of superconducting oscillating components of different symmetry compared to the bulk one developing in the superconducting side. Guided by this motivation, a particular attention has been devoted to the differences arising in the system when the two distinct mechanisms for ferromagnetism are separately taken under consideration. We stress that for both mechanisms the manifestation of these effects is intimately related to the presence of an anisotropic superconductor facing the ferromagnet. Actually, when a conventional s-wave $S-F$ junction is considered, one can only observe the formation of a subdominant anisotropic s-wave component, characterized by a very small amplitude compared to the dominant one. This holds regardless of the mechanism of generation of the ferromagnetism. Nevertheless, even in such a conventional case there are differences emerging in the density of states at the interface. Indeed, the dip-peak-like features of the DOS for the Stoner mechanism are energy dependent and they shift from negative to positive frequencies if the exchange amplitude is varied toward the half-metallic regime. On the contrary, in the case of spin bandwidth asymmetry the DOS for the spin majority carriers exhibits an asymmetric profile at all values of the ratio $t_{F\downarrow}/t_{F\uparrow}$, with a dip (peak) structure at negative (positive) values of the energy. On the other hand, the DOS for the spin minority channel does not change significantly in the energy range that is relevant for the superconducting pairing.

We point out that the analysis here has been confined to the high-transparency case. Nonetheless, the analysis of junctions with low-transparent interfaces also deserves great attention, given that in real systems the difference in the electronic structure between the ferromagnet and the superconductor tends to give rise to a potential barrier at the interface. Moreover, in the low-transparency limit significant differences emerge between the two cases of chiral p-wave and d-wave symmetry, due to the fact that midgap Andreev resonant states play a fundamental role in the former and are absent in the latter. This is evident from the formation in the p-wave case of a zero-energy peak in the local DOS at the interface, which tends to disappear as the transparency of the barrier is gradually increased.[14] On the other hand, a similar effect is not seen in d-wave junctions.[8]

To further investigate the proximity effect in our F/US bilayer junction, we have also concentrated our attention on a relevant experimentally accessible quantity, the local density of states. A detailed analysis has been performed, in particular, as concerns the effects introduced at the interface by the anisotropy of the superconducting order parameters. The differences already pointed out associated with the two kinds of ferromagnetism considered here manifest themselves in peculiar behaviors of the density of states at the interface, in the p-wave case, as well as in the d-wave case,

with distinct effects on the opening of gaplike structures in the DOS of both kinds of spin species. We believe that these effects can turn out to be of special relevance in the determination of the transport properties, which are expected to exhibit specific and unconventional features, in particular when one moves toward the half-metal regime. A study in this direction, specifically concentrated on the analysis of the differential conductance, is in progress and will be the subject of a forthcoming paper.

ACKNOWLEDGMENT

We kindly thank S. Bergeret for useful and fruitful discussions.

[1] G. Deutscher and P. G. de Gennes, in *Superconductivity*, edited by R. D. Parks (Dekker, New York, 1969), Vol. 2, p. 1005.
[2] B. Pannetier and H. Courtois, J. Low Temp. Phys. **118**, 599 (2000).
[3] E. A. Demler, G. B. Arnold, and M. R. Beasley, Phys. Rev. B **55**, 15174 (1997).
[4] K. Halterman and O. T. Valls, Phys. Rev. B **65**, 014509 (2001); **66**, 224516 (2002).
[5] Z. Radović, M. Ledvij, L. Dobrosavljević-Grujić, A. I. Buzdin, and J. R. Clem, Phys. Rev. B **44**, 759 (1991).
[6] V. V. Ryazanov, V. A. Oboznov, A. Yu. Rusanov, A. V. Veretennikov, A. A. Golubov, and J. Aarts, Phys. Rev. Lett. **86**, 2427 (2001); T. Kontos, M. Aprili, J. Lesueur, F. Genêt, B. Stephanidis, and R. Boursier, *ibid.* **89**, 137007 (2002); H. Sellier, C. Baraduc, F. Lefloch, and R. Calemczuk, Phys. Rev. B **68**, 054531 (2003).
[7] C.-R. Hu, Phys. Rev. Lett. **72**, 1526 (1994); J. Yang and C.-R. Hu, Phys. Rev. B **50**, 16766 (1994).
[8] Y. Tanaka and S. Kashiwaya, Phys. Rev. Lett. **74**, 3451 (1995).
[9] M. Fogelström, D. Rainer, and J. A. Sauls, Phys. Rev. Lett. **79**, 281 (1997).
[10] M. Covington, M. Aprili, E. Paraoanu, L. H. Greene, F. Xu, J. Zhu, and C. A. Mirkin, Phys. Rev. Lett. **79**, 277 (1997); J. Y. T. Wei, N.-C. Yeh, D. F. Garrigus, and M. Strasik, *ibid.* **81**, 2542 (1998).
[11] F. Laube, G. Goll, H. v. Löhneysen, M. Fogelström, and F. Lichtenberg, Phys. Rev. Lett. **84**, 1595 (2000); Z. Q. Mao, K. D. Nelson, R. Jin, Y. Liu, and Y. Maeno, *ibid.* **87**, 037003 (2001).
[12] Ch. Wälti, H. R. Ott, Z. Fisk, and J. L. Smith, Phys. Rev. Lett. **84**, 5616 (2000).
[13] S. Kashiwaya, Y. Tanaka, M. Koyanagi, and K. Kajimura, Phys. Rev. B **53**, 2667 (1996).
[14] Y. Tanuma, Y. Tanaka, and S. Kashiwaya, Phys. Rev. B **74**, 024506 (2006).
[15] Y. Tanaka, Yu. V. Nazarov, and S. Kashiwaya, Phys. Rev. Lett. **90**, 167003 (2003); Y. Tanaka, Yu. V. Nazarov, A. A. Golubov, and S. Kashiwaya, Phys. Rev. B **69**, 144519 (2004).
[16] Y. Tanaka and S. Kashiwaya, Phys. Rev. B **70**, 012507 (2004); Y. Tanaka, S. Kashiwaya, and T. Yokoyama, *ibid.* **71**, 094513 (2005).
[17] Y. Tanaka, Y. Tanuma, K. Kuroki, and S. Kashiwaya, J. Phys. Soc. Jpn. **71**, 2102 (2002); Y. Tanuma, K. Kuroki, Y. Tanaka, R. Arita, S. Kashiwaya, and H. Aoki, Phys. Rev. B **66**, 094507 (2002).
[18] S. Kashiwaya, Y. Tanaka, N. Yoshida, and M. R. Beasley, Phys. Rev. B **60**, 3572 (1999).
[19] I. Zutić and O. T. Valls, Phys. Rev. B **60**, 6320 (1999); **61**, 1555 (2000).
[20] J.-X. Zhu and C. S. Ting, Phys. Rev. B **61**, 1456 (2000).
[21] N. Stefanakis and R. Mélin, J. Phys.: Condens. Matter **15**, 3401 (2003).
[22] J. Linder and A. Sudbø, Phys. Rev. B **75**, 134509 (2007).
[23] N. Stefanakis and R. Mélin, J. Phys.: Condens. Matter **15**, 4239 (2003).
[24] An exhaustive presentation of the most relevant results on the proximity effect in N-S and F-S heterostructures can be found in G. Deutscher, Rev. Mod. Phys. **77**, 109 (2005); A. I. Buzdin, *ibid.* **77**, 935 (2005); F. S. Bergeret, A. F. Volkov, and K. B. Efetov, *ibid.* **77**, 1321 (2005).
[25] J. M. D. Coey and M. Venkatesan, J. Appl. Phys. **91**, 8345 (2002).
[26] M. I. Katsnelson, V. Yu. Irkhin, L. Chioncel, A. I. Lichtenstein, and R. A. de Groot, Rev. Mod. Phys. **80**, 315 (2008).
[27] C. Zener, Phys. Rev. **82**, 403 (1951); P. W. Anderson and H. Hasegawa, *ibid.* **100**, 675 (1955).
[28] J. E. Hirsch, Phys. Rev. B **40**, 2354 (1989); J. E. Hirsch, *ibid.* **40**, 9061 (1989); J. E. Hirsch, *ibid.* **59**, 6256 (1999).
[29] Y. Okimoto, T. Katsufuji, T. Ishikawa, A. Urushibara, T. Arima, and Y. Tokura, Phys. Rev. Lett. **75**, 109 (1995); Y. Okimoto, T. Katsufuji, T. Ishikawa, T. Arima, and Y. Tokura, Phys. Rev. B **55**, 4206 (1997).
[30] L. Degiorgi, E. Felder, H. R. Ott, J. L. Sarrao, and Z. Fisk, Phys. Rev. Lett. **79**, 5134 (1997); S. Broderick, B. Ruzicka, L. Degiorgi, H. R. Ott, J. L. Sarrao, and Z. Fisk, Phys. Rev. B **65**, 121102(R) (2002).
[31] E. J. Singley, K. S. Burch, R. Kawakami, J. Stephens, D. D. Awschalom, and D. N. Basov, Phys. Rev. B **68**, 165204 (2003); E. J. Singley, R. Kawakami, D. D. Awschalom, and D. N. Basov, Phys. Rev. Lett. **89**, 097203 (2002).
[32] R. Fittipaldi, A. Vecchione, R. Ciancio, S. Pace, M. Cuoco, D. Stornaiuolo, D. Born, F. Tafuri, E. Olsson, S. Kittaka, H. Yaguchi, and Y. Maeno, Europhys. Lett. **83**, 27007 (2008).
[33] M. Cuoco, P. Gentile, and C. Noce, Phys. Rev. Lett. **91**, 197003 (2003).
[34] R. S. Keizer, S. T. B. Goennenwein, T. M. Klapwijk, G. Miao, G. Xiao, and A. Gupta, Nature (London) **439**, 825 (2006); Y. Asano, Y. Tanaka, and A. A. Golubov, Phys. Rev. Lett. **98**, 107002 (2007); V. Braude and Y. V. Nazarov, *ibid.* **98**, 077003 (2007); M. Eschrig, J. Kopu, J. C. Cuevas, and G. Schon, *ibid.* **90**, 137003 (2003).
[35] K. Kuboki and H. Takahashi, Phys. Rev. B **70**, 214524 (2004).
[36] M. Matsumoto and H. Shiba, J. Phys. Soc. Jpn. **64**, 3384 (1995) **64**, 4867 (1995).
[37] M. Matsumoto and M. Sigrist, J. Phys. Soc. Jpn. **68**, 994 (1999).
[38] R. Micnas, J. Ranninger, and S. Robaszkiewicz, Rev. Mod. Phys. **62**, 113 (1990).

[39] K. Kuboki, J. Phys. Soc. Jpn. **70**, 2698 (2001).
[40] See the review paper by Bergeret, Volkov, and Efetov cited in Ref. 24.
[41] F. S. Bergeret, A. F. Volkov, and K. B. Efetov, Phys. Rev. Lett. **86**, 4096 (2001).
[42] F. S. Bergeret, A. F. Volkov, and K. B. Efetov, Phys. Rev. B **68**, 064513 (2003).
[43] K. Halterman, P. H. Barsic, and O. T. Valls, Phys. Rev. Lett. **99**, 127002 (2007).
[44] R. Fazio and C. Lucheroni, Europhys. Lett. **45**, 707 (1999).
[45] I. Baladié and A. Buzdin, Phys. Rev. B **64**, 224514 (2001).
[46] K. Kuboki, J. Phys. Soc. Jpn. **68**, 3150 (1999).
[47] R. Wiesendanger, H.-J. Güntherodt, G. Güntherodt, R. J. Gambino, and R. Ruf, Phys. Rev. Lett. **65**, 247 (1990); M. Kleiber, M. Bode, R. Ravlic, and R. Wiesendanger, *ibid.* **85**, 4606 (2000).
[48] S. Heinze, M. Bode, A. Kubetzka, O. Pietzsch, X. Nie, S. Blügel, and R. Wiesendanger, Science **288**, 1805 (2000).
[49] M. Bode, Rep. Prog. Phys. **66**, 523 (2003).